JOURNAL OF PROPULSION AND POWER
Vol. 13, No. 1, January–February 1997

Comparison Between Presumed and Monte Carlo Probability Density Function Combustion Models

Fernando Biagioli*
Centre for Advanced Studies, Research, and Development in Sardinia, Cagliari 09123, Italy

The presumed probability density function (PDF) and PDF transport methods are applied to the simulation of two H_2/CO/N_2–air nonpremixed turbulent flames for which experimental data are available. The thermochemical model is based on a one-step reduced reaction mechanism accounting for the finite rate kinetics of the free-radicals slow recombinations. A mixed finite volume/Monte Carlo technique is used to solve the composition PDF transport equation; this technique is coupled with a two-dimensional finite volume multiblock flow solver that provides the mean velocity, pressure, and eddy viscosity fields. The convective terms in the conservation equations for the momentum components are approximated via a second-order total variation diminishing scheme; it is shown that on coarse grids this scheme performs more accurately than the classical first-order hybrid scheme. Comparable results between the presumed PDF and PDF transport methods are observed.

Nomenclature

c_j = species concentration
c_μ = eddy viscosity coefficient
d = fuel inlet diameter
f = mixture fraction
I = unit tensor
k = turbulent kinetic energy
N = number of particles
ni = number of cells in the x direction
nj = number of cells in the y direction
P = probability density function
p = static pressure
r = normalized progress variable
S = stress tensor
T = temperature
T_a = activation temperature
$\boldsymbol{u}$ = velocity vector
W_j = species molecular weights
w_r = chemical source term of progress variable
Y_j = species mass fractions
Y^* = progress variable
ε = dissipation of turbulent kinetic energy
μ_t = eddy viscosity
ρ = density
σ_t = turbulent Prandtl number
τ_f = decay time of mixture fraction variance
$\bar{}$ = conventional averaging
$\tilde{}$ = Favre averaging

Introduction

THE simulation of turbulent reacting flows of engineering interest will continue to rely for a long time on methods based on the determination of statistical moments.

Beside the need to provide a closure for the turbulent transport of momentum, energy, and species concentrations, a second important closure problem, the turbulence-chemistry interaction, arises in the presence of combustion.

In fact, for a simple bimolecular reaction $A + B \rightarrow C$, expanding the reaction rate $w = A \exp(-T_a/T)c_A c_B$ via a Taylor series expansion and time averaging, the result is[1]

$$\bar{w} = A \exp(-T_a/\tilde{T})\overline{c_A c_B}\left[1 + \left(\frac{T_a^2}{\tilde{T}^2} - 2\frac{T_a}{\tilde{T}}\right)\frac{\overline{T''^2}}{\tilde{T}^2} + \frac{T_a}{\tilde{T}}\left(\frac{\overline{T''c_A''}}{\tilde{T}\,\tilde{c}_A} + \frac{\overline{T''c_B''}}{\tilde{T}\,\tilde{c}_B}\right) + \cdots\right] \quad (1)$$

This series converges very slowly[2] because of $T_a/\tilde{T} >> 1$ for most combustion reactions; an impressive number of correlations should therefore be modeled.

An alternative way to calculate the statistical moments of any thermochemical quantity consists of directly determining the composition probability density function (PDF); for this purpose, two methods have been extensively used during the last two decades, both for premixed and nonpremixed combustion modeling:

1) Using a PDF of a presumed shape parametrized with respect to first- and second-order moments of the independent thermochemical variables.

2) Determining the PDF from a modeled transport equation.

Because of the chemical source term appearing in closed form, methods based on the transport equation for the composition PDF are often claimed to be superior to presumed PDF methods. In both of these methods closures for the turbulent transport and the molecular dissipation of scalars correlations have to be provided. Concerning turbulent transport, a gradient diffusion assumption, where the eddy diffusivity is assumed proportional to the eddy viscosity used in the momentum equation, works sufficiently well in shear flows; the molecular dissipation of scalars correlations, instead, is often considered proportional[3] to the dissipation of the turbulent kinetic energy, a reasonable assumption in the distributed combustion regime.

The purpose of this paper is to compare the presumed PDF and the PDF transport methods applied to the simulation of two H_2/CO/N_2–air nonpremixed turbulent flames for which experimental data are available.[4,5] The study of the oxidation of H_2/CO fuels is very important because H_2 and CO are intermediate products in hydrocarbons combustion.

A reduction in the number of independent thermochemical variables (without losing the essential features of finite rate combustion) is necessary to limit the computational and modeling effort of PDF methods; here, the thermochemical model

Received Aug. 3, 1995; revision received March 18, 1996; accepted for publication April 26, 1996.

*Research Engineer. Member AIAA.

Table 1 Reaction mechanism for $H_2/CO/N_2$–air combustion[a]

No.	Reaction	A	β	E
(R1)	$H + O_2 \rightleftharpoons OH + O$	2.00E14	0.0	16,800
(R2)	$O + H_2 \rightleftharpoons OH + H$	5.06E04	2.67	6,290
(R3)	$H_2 + OH \rightleftharpoons H_2O + H$	1.17E09	1.3	3,626
(R4)	$OH + OH \rightleftharpoons H_2O + O$	6.00E08	1.3	0
(R5)	$CO + OH \rightleftharpoons CO_2 + H$	1.51E07	1.3	−758
(R6)	$H + OH + M \rightleftharpoons H_2O + M$ Third-body efficiencies: $H_2O = 5.0$	1.60E22	−2.0	0
(R7)	$H + O + M \rightleftharpoons OH + M$ Third-body efficiencies: $H_2O = 5.0$	6.20E16	−0.6	0
(R8)	$H + H + M \rightleftharpoons H_2 + M$ Third-body efficiencies: $H_2 = 0.0$, $H_2O = 0.0$, $CO_2 = 0.0$	1.00E18	−1.0	0
(R9)	$O + O + M \rightleftharpoons O_2 + M$	1.89E13	0.0	−1,788

[a]Rate coefficients in the form $k = AT^{\beta} \exp(-E/RT)$. Units are centimeters, molecules, seconds, Kelvin, and calories.

is based on a one-step reduced kinetics mechanism[6] (only two independent variables: the mixture fraction and a kinetics progress variable), where all reactions are in partial equilibrium except the three-body slow recombinations of free radicals (see Table 1).

The PDF transport equation can, in principle, be solved via finite volume or finite difference techniques but, unfortunately, the associated computational effort increases exponentially with the number of independent variables; therefore, Monte Carlo simulation methods are preferred, their computational effort growing only linearly.

The transport equation for the composition PDF has been solved in this work with a mixed finite volume/Monte Carlo technique,[7] coupled with a two-dimensional multiblock finite volume code in Cartesian/cylindrical coordinates developed by the author,[8] which provides the mean velocity, pressure, and other relevant quantities like k and ε.

Because of the low Mach number at which turbulent combustion takes place, mass conservation is satisfied solving a Poisson-like equation for the pressure correction[9] (SIMPLE algorithm). To avoid the pressure-velocity decoupling arising from the discretization of pressure gradients via central differencing, a staggered grid arrangement for the velocity components is generally employed. In this work a nonstaggered grid arrangement has been successfully used eliminating the decoupling via the Rhie and Chow interpolation[10] of the convective terms on cells boundaries. The use of nonstaggered grids is very convenient because it simplifies the implementation of boundary conditions, especially at the block interfaces in the case of multiblock decomposition of the flowfield.

Finally, two discretization schemes have been used for the convective terms in the momentum equations: a second-order TVD scheme proposed by Jones[11] and the classical first-order hybrid scheme.[9]

Presumed PDF and PDF transport methods have only rarely[12,13] been compared. For this reason, an extensive comparison between these methods will be presented.

Governing Equations

Conservation Equations

The following averaged transport equations have to be solved for mass and momentum:

$$\frac{\partial \bar{\rho}}{\partial t} + \nabla \cdot (\bar{\rho} \tilde{\boldsymbol{u}}) = 0 \tag{2}$$

$$\frac{\partial (\bar{\rho} \tilde{\boldsymbol{u}})}{\partial t} + \nabla \cdot (\bar{\rho} \tilde{\boldsymbol{u}} \tilde{\boldsymbol{u}}) = -\nabla \bar{p} + \nabla \cdot (\bar{S} - \bar{\rho} \widetilde{\boldsymbol{u}''\boldsymbol{u}''}) \tag{3}$$

where Favre averaging is used.

Turbulent transport has been modeled with the standard k-ε model[14]:

$$-\bar{\rho} \widetilde{\boldsymbol{u}''\boldsymbol{u}''} = 2\mu_t \left[\frac{\nabla \tilde{\boldsymbol{u}} + (\nabla \tilde{\boldsymbol{u}})^T}{2} - \frac{1}{3} (\nabla \cdot \tilde{\boldsymbol{u}}) \boldsymbol{I} \right] - \frac{2}{3} \bar{\rho} k \boldsymbol{I}$$
$$\mu_t = c_\mu \tilde{\rho} \frac{k^2}{\varepsilon}, \qquad c_\mu = 0.09 \tag{4}$$

where k and ε are determined from the following modeled conservation equations:

$$\frac{\partial (\bar{\rho} k)}{\partial t} + \nabla \cdot (\bar{\rho} \tilde{\boldsymbol{u}} k) = \nabla \cdot \left(\frac{\mu_t}{\sigma_k} \nabla k \right) - \bar{\rho} \widetilde{\boldsymbol{u}''\boldsymbol{u}''} : \nabla \tilde{\boldsymbol{u}} - \bar{\rho} \varepsilon \tag{5}$$

$$\frac{\partial (\bar{\rho} \varepsilon)}{\partial t} + \nabla \cdot (\bar{\rho} \tilde{\boldsymbol{u}} \varepsilon) = \nabla \cdot \left(\frac{\mu_t}{\sigma_\varepsilon} \nabla \varepsilon \right) - c_1 \frac{\varepsilon}{k} (\bar{\rho} \widetilde{\boldsymbol{u}''\boldsymbol{u}''} : \nabla \tilde{\boldsymbol{u}}) - c_2 \bar{\rho} \frac{\varepsilon^2}{k} \tag{6}$$

with $c_1 = 1.44$, $c_2 = 1.92$, $\sigma_k = 1.0$, and $\sigma_\varepsilon = 1.3$.

Reduced Reaction Mechanism

The combustion of $H_2/CO/N_2$–air mixtures can be reasonably described by the simple reaction mechanism reported in Table 1, where N_2 has been considered as a passive diluent.

To limit the computational and modeling effort of PDF methods, a reduction in the number of independent thermochemical scalars is strongly recommended. To do this, partial equilibrium[6] is assumed here for the fast two-body shuffle reactions R1–R5, an assumption that has been found valid by Warnatz[15] for temperatures above 1500 K, whereas finite rate chemistry is retained for the slow three-body recombinations R6–R9 of free radicals O, OH, and H.

In this case all of the thermochemical quantities can be expressed as functions of only two scalars, f and Y^*, accounting for the progress of reactions R6–R9 and given by

$$Y^* = Y_{H_2} + \frac{W_{H_2}}{W_{CO}} Y_{CO} + \frac{3}{2} \frac{W_{H_2}}{W_H} Y_H + \frac{W_{H_2}}{W_O} Y_O + \frac{1}{2} \frac{W_{H_2}}{W_{OH}} Y_{OH} \tag{7}$$

Therefore,

$$\rho, T, Y_j = F(f, Y^*) \tag{8}$$

For reasons that will be made clear in the next section, it is convenient to normalize Y^* with its maximum and minimum values given, respectively, by the frozen and equilibrium states of reactions R6–R9:

$$r = \frac{Y^* - Y^{*,(\mathrm{fr})}(f)}{Y^{*,(\mathrm{eq})}(f) - Y^{*,(\mathrm{fr})}(f)} \tag{9}$$

Here, all of the dependent thermochemical quantities ρ, T, and Y_j have been determined by minimizing the Gibbs free energy via the Lagrange multipliers method,[16] subject to the constraint of fixed values for f and Y^*.

Presumed PDF Method

The system of Eqs. (2) and (3) is closed with a PDF-based combustion model, which provides the mean density $\bar{\rho}$ and the statistical average $\tilde{\phi}$ (or $\bar{\phi}$) of any other relevant thermochemical quantity:

$$\bar{\rho} = \left[\int_0^1 \int_{Y^{*,(\mathrm{eq})}(f)}^{Y^{*,(\mathrm{fr})}(f)} \frac{\tilde{P}(f, Y^*)}{\rho(f, Y^*)} \, \mathrm{d}Y^* \, \mathrm{d}f \right]^{-1} \tag{10}$$

$$\tilde{\phi} = \int_0^1 \int_{Y^{*,(\mathrm{eq})}(f)}^{Y^{*,(\mathrm{fr})}(f)} \tilde{P}(f, Y^*) \phi(f, Y^*) \, \mathrm{d}Y^* \, \mathrm{d}f \tag{11}$$

$$\bar{\phi} = \bar{\rho} \, (\widetilde{\phi/\rho}) \tag{12}$$

$\tilde{P}(f, Y^*) = \rho(f, Y^*)P(f, Y^*)/\bar{\rho}$ being the Favre PDF between the two independent thermochemical variables.

Following Janicka and Kollmann,[17] a double β function, parametrized with respect to first- and second-order moments of f and r, is assumed here for the Favre PDF:

$$\tilde{P}(f, r) = P_\beta(f, \tilde{f}, \widetilde{f''^2}) P_\beta(r, \tilde{r}, \widetilde{r''^2}) \tag{13}$$

$$P_\beta(\xi, \tilde{\xi}, \widetilde{\xi''^2}) = \frac{\xi^{a_\xi - 1}(1 - \xi)^{b_\xi - 1}}{\int_0^1 \xi^{a_\xi - 1}(1 - \xi)^{b_\xi - 1} \, \mathrm{d}\xi} \tag{14}$$

$$a_\xi = \tilde{\xi} \left[\frac{\tilde{\xi}(1 - \tilde{\xi})}{\widetilde{\xi''^2}} - 1 \right] \tag{15}$$

$$b_\xi = (1 - \tilde{\xi}) \left[\frac{\tilde{\xi}(1 - \tilde{\xi})}{\widetilde{\xi''^2}} - 1 \right] \tag{16}$$

where ξ indicates f and r indifferently. The model is completed by the following conservation equations for the mean and variance of the two thermochemical variables:

$$\frac{\partial(\bar{\rho}\tilde{f})}{\partial t} + \nabla \cdot (\bar{\rho}\tilde{\boldsymbol{u}}\tilde{f}) = \nabla \cdot \left(\frac{\mu_t}{\sigma_t} \nabla f \right) \tag{17}$$

$$\frac{\partial(\bar{\rho}\widetilde{f''^2})}{\partial t} + \nabla \cdot (\bar{\rho}\tilde{\boldsymbol{u}}\widetilde{f''^2}) = \nabla \cdot \left(\frac{\mu_t}{\sigma_t} \nabla \widetilde{f''^2} \right) + 2 \frac{\mu_t}{\sigma_t} |\nabla \tilde{f}|^2 - C_D \bar{\rho} \frac{\widetilde{f''^2}}{k} \varepsilon \tag{18}$$

$$\frac{\partial(\bar{\rho}\tilde{r})}{\partial t} + \nabla \cdot (\bar{\rho}\tilde{\boldsymbol{u}}\tilde{r}) = \nabla \cdot \left(\frac{\mu_t}{\sigma_t} \nabla \tilde{r} \right) + \overline{w_r} + C_D \bar{\rho} \tilde{r} \frac{\varepsilon}{k} \widetilde{\frac{1}{W} \frac{\mathrm{d}^2 W}{\mathrm{d}f^2}} \widetilde{f''^2} \tag{19}$$

$$\frac{\partial(\bar{\rho}\widetilde{r''^2})}{\partial t} + \nabla \cdot (\bar{\rho}\tilde{\boldsymbol{u}}\widetilde{r''^2}) = \nabla \cdot \left(\frac{\mu_t}{\sigma_t} \nabla \widetilde{r''^2} \right) + 2 \frac{\mu_t}{\sigma_t} |\nabla \tilde{r}|^2 + 2\overline{r'' w_r} - 2\bar{\rho} C_D \frac{\varepsilon}{k} \widetilde{r''^2} \left(1 - \widetilde{f''^2} \widetilde{\frac{1}{W} \frac{\mathrm{d}^2 W}{\mathrm{d}f^2}} \right) \tag{20}$$

where $W = Y^{*,(\mathrm{eq})}(f) - Y^{*,(\mathrm{fr})}(f)$, $\sigma_t = 0.7$, and $C_D = 2$.

PDF Transport Method

A transport equation for the composition PDF, $\tilde{P}(f, Y^*, \boldsymbol{x}, t)$, can be obtained exactly[3] in a form where turbulent transport and the molecular mixing terms responsible for the dissipation of scalars fluctuations (the terms inside brackets) have to be modeled:

$$\frac{\partial(\bar{\rho}\tilde{P})}{\partial t} + \nabla \cdot [\bar{\rho}(\tilde{\boldsymbol{u}} + \langle \boldsymbol{u}'' | f, Y^* \rangle)\tilde{P}] = -\frac{\partial^2}{\partial Y^{*2}} \left(\langle \rho D |\nabla Y^*|^2 | f, Y^* \rangle \frac{\bar{\rho}}{\rho} \tilde{P} \right) - \frac{\partial}{\partial Y^*} \left(\frac{w}{\rho} \bar{\rho}\tilde{P} \right) - \frac{\partial^2}{\partial f^2} \left(\langle \rho D |\nabla f|^2 | f, Y^* \rangle \frac{\bar{\rho}}{\rho} \tilde{P} \right) \tag{21}$$

The symbol $\langle | \rangle$ indicates conditional averaging.

A standard eddy diffusivity model has been employed to close the turbulent transport:

$$-(\bar{\rho}\langle \boldsymbol{u}'' | f, Y^* \rangle \tilde{P}) = (\mu_t/\sigma_t) \nabla \tilde{P} \tag{22}$$

The molecular mixing term has been modeled via the linear mean square estimation (LMSE) model by Dopazo[18] (reported here only for f, being analogous for Y^*):

$$-\frac{\partial^2}{\partial f^2} \left(\langle \rho D |\nabla f|^2 | f, Y^* \rangle \frac{\bar{\rho}}{\rho} \tilde{P} \right) = \frac{\partial}{\partial f} \left(\frac{1}{2} \frac{f - \tilde{f}}{\tau_f} \bar{\rho}\tilde{P} \right) \tag{23}$$

with the characteristic decay time of scalars fluctuations assumed proportional to the turbulent kinetic energy decay time ($\tau_f = \tau/C_D$, $\tau = k/\varepsilon$) consistent with the $\widetilde{f''^2}$ transport equation in the presumed PDF method.

Numerical Method

Finite Volume Method

The transport equations for mass, momentum, k, ε, and the statistical moments of the two independent thermochemical variables in the presumed PDF method have been solved via the finite volume method.

Because of the low Mach number at which combustion takes place, the pressure is determined by solving a Poisson-like equation (SIMPLE algorithm). Density instead is calculated from the equation of state.

The code used[8] is a multiblock two-dimensional planar/axisymmetric in Cartesian/cylindrical coordinates based on a nonstaggered grid arrangement. To avoid the pressure–velocity decoupling that may arise because of the nonstaggered grid,[9] the convective terms on cells boundaries have been calculated with the Rhie and Chow interpolation.[10] The nonstaggered grid arrangement is more efficient and simpler for implementing boundary conditions, especially at blocks interfaces where two rows of cells overlap because of the Rhie and Chow interpolation.[10]

Two discretization schemes have been tested to approximate the convective fluxes at the cell boundaries: 1) the hybrid upwind-central scheme[9] (first-order accurate) and 2) a second-order TVD scheme suggested by Jones.[11] The application of the TVD scheme is limited only to the velocity components.

Monte Carlo Method

In principle, the solution of the PDF transport equation by finite difference is feasible, but too expensive, from a computational point of view. The computational efforts of finite difference, in fact, increase exponentially with the dimensionality of the PDF equation[3]; the computational effort of Monte Carlo methods instead rises only linearly.[7]

In this work a mixed finite volume/Monte Carlo method has been developed starting from that of Pope.[7] This approach has

the advantages of the Monte Carlo algorithm and, at the same time, the simplicity and robustness of the finite volume technique.

The convective and diffusive operators in PDF Eq. (21) are discretized with the finite volume method and rearranged in the standard form:

$$\tilde{P}_P(t+\Delta t) = \tilde{P}_P(t) - A_P \Delta t \tilde{P}_P(t) + \Delta t \underbrace{\sum_{\alpha=W,E,S,N} A_\alpha \tilde{P}_\alpha(t)}_{[CD]\cdot\{\tilde{P}\}(t)}$$

$$+ \Delta t \frac{\partial}{\partial f}\left[\frac{f-\tilde{f}_P}{k/\varepsilon}\bar{\rho}_P \tilde{P}_P(t)\right] + \Delta t \frac{\partial}{\partial Y^*}\left[\left(\frac{Y^* - \widetilde{Y^*}_P}{k/\varepsilon} - \frac{w}{\rho}\right)\bar{\rho}_P \tilde{P}_P(t)\right]$$

$$\underbrace{\qquad\qquad}_{[CM]\cdot\{\tilde{P}\}(t)} \tag{24}$$

where [CD] is the convective–diffusive operator (transport in the physical space) and [CM] is the chemical plus molecular mixing operator (transport in the composition space), which has been left unchanged.

In the present work, Eq. (24) is split in the product of these two operators:

$$\{\tilde{P}\}(t+\Delta t) = ([I] + [CM])\cdot([I] + [CD])\cdot\{\tilde{P}\}(t) \tag{25}$$

Pope's approach is based instead on the separate splitting of the [CD] operator in the convective and diffusive parts in each direction (four distinct operators for two-dimensional problems).

The PDF at each point of the finite volume grid is approximated with a set of N representative values $\{[f^{(p)}, Y^{*(p)}], p = 1, 2, \ldots, N\}$ of the composition (denoted particles). To satisfy the equivalence condition stated by Pope,[7] i.e., that the ensemble average $\tilde{\phi}_N$ of any dependent thermochemical quantity $\phi(f, Y^*)$ converges to the exact average $\tilde{\phi}$ [the one satisfying Eq. (24)] when $N \to \infty$

$$\lim_{N\to\infty} \tilde{\phi}_N = \lim_{N\to\infty} \frac{1}{N}\sum_{p=1}^{N} \phi[\hat{f}^{(p)}, \hat{n}^{(p)}] = \tilde{\phi} \tag{26}$$

the sets of particles are made to evolve in the physical and composition space in the following ways:

1) Convection and diffusion. The set of representative values of the PDF at node P and at time $t + \Delta t$ is created by randomly selecting particles from node P itself and from the adjacent nodes W, E, S, and N at time t in amounts proportional to the influence coefficients A_P and A_α.

2) Chemistry and molecular dissipation. Each particle is moved in the composition space according to

$$f^{(p)}(t+\Delta t) = f^{(p)}(t) - \Delta t \bar{\rho}\frac{f^{(p)}(t) - \tilde{f}}{k/\varepsilon} \tag{27}$$

$$Y^{*(p)}(t+\Delta t) = Y^{*(p)}(t) - \Delta t \bar{\rho}\left[\frac{Y^{*(p)}(t) - \widetilde{Y^*}}{k/\varepsilon} - \frac{w}{\rho}\right] \tag{28}$$

A large number of particles has to be used to limit the large statistical error of Monte Carlo methods (the error $\simeq N^{-1/2}$). In this work each cell of the finite volume grid has 100 particles. To further reduce the statistical error, the number of actual particles has been increased by time averaging each thermochemical variable over 100 time steps.

The conventional way to define the residual error in the finite volume method is meaningless in the Monte Carlo simulation, because its statistical error is generally larger than the truncation error when using finite volume for the statistical moments of the presumed PDF method. The residual error for any averaged thermochemical quantity $\bar{\phi}$ is defined here as

$$\text{err} = \frac{1}{ni \times nj}\sum_{ij}\frac{[\bar{\phi}_{ij}(t+\Delta t) - \bar{\phi}_{ij}(t)]^2}{[\bar{\phi}_{ij}(t)]^2} \tag{29}$$

This error doesn't converge to zero as in the finite volume method, but rather to a value representative of the statistical fluctuation of the solution when steady state is reached; this level depends on the number of particles in each cell and on the number of time steps over which the solution is averaged. The value of err = 10^{-5} has been reached in the present calculations.

Results

Description of the Test Cases

The presumed PDF and PDF transport methods have been tested in simulations of two axisymmetric $H_2/CO/N_2$–air nonpremixed turbulent flames for which experimental data are available.[4,5]

The experimental apparatus is schematically reproduced in Fig. 1; the fuel molar composition and the inlet conditions are also reported. A circular fuel injector is centered in a 15-cm^2 test section; flame A[4] is characterized by a little axisymmetrical flameholder around the fuel injector that is not present in flame B.[5]

Axial velocities were measured with a dual-beam, real fringe laser Doppler velocimetry (LDV), whereas temperature, major species concentrations (H_2, O_2, CO, H_2O, and OH), density, and mixture fraction were determined simultaneously using pulsed Raman scattering. The accuracy reported for the Raman measurements is ±50 K for temperature and ±1 mole % for H_2, O_2, CO, and H_2O concentrations in the case of H_2–air flames. It is argued by the authors of the experiments that in the case of $H_2/CO/N_2$–air flames the accuracy deteriorates because of the presence of CO in the fuel. Finally, the accuracy of the OH measurements is ±30%.

Comparison with Experiments

Since in both cases the flame is confined in a small region near the centerline, all of the calculations have been performed axisymmetrically in a circular duct with the same cross-sectional area of the square channel of the experiments.

Flame A

To test the dependence of the results from the mesh size, a simulation of flame A has been performed with the presumed

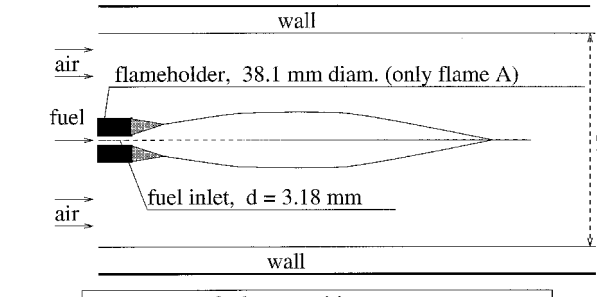

fuel composition	CO	H2	N2
Flame A	27.5%	32.3%	40.2%
Flame B	40.0%	30.0%	30.0%

	Uair	Tair	Ufuel	Tfuel	pressure
Flame A	6.5 m/s	300 K	80.0 m/s	300 K	1 atm
Flame B	2.4 m/s	300 K	54.6 m/s	300 K	1 atm

Fig. 1 Schematic of the combustor and inlet conditions.

PDF model for two different meshes, the coarser of which is shown in Fig. 2; three blocks have been used to also include the fuel and air inlets in the solution domain.

Figure 3 shows the streamlines in the recirculation zone behind the flameholder obtained with the first-order hybrid scheme (upper half) and the second-order total variation diminishing (TVD) scheme (lower half) on the two meshes. The use of the second-order TVD scheme on the fine mesh gives the maximum length for the recirculation zone ($\simeq 11.5d$) because of the minimum amount of numerical diffusion introduced; the first-order hybrid scheme on the coarse mesh, which introduces the maximum amount of numerical diffusion, gives instead the shorter recirculation zone ($\simeq 8.5d$). The second-order TVD scheme on the coarse mesh and the first-order scheme on the fine mesh both give a length of $\simeq 10.5d$ for the recirculation zone, only $1d$ shorter than the one obtained with the second-order TVD scheme on the fine mesh; therefore, taking the solution obtained with the second-order TVD scheme on the fine mesh as the reference, the results obtained with the first-order scheme on the fine mesh and the second-order TVD scheme on the coarse mesh are reasonably accurate. On the contrary, using the first-order scheme on the coarse mesh cannot guarantee acceptable accuracy. On the basis of these results, all of the calculations hereafter have been performed with the TVD scheme on the coarse grid; the use of the coarse grid, in fact, saves a large amount of CPU time and computer storage when running the Monte Carlo algorithm, whereas the use of the TVD scheme guarantees nearly grid-independent results.

CPU time to obtain the solution on a workstation IBM RISC6000 model 580 was about 30 min in the case of the presumed PDF method, and 10 h in the case of the PDF transport method.

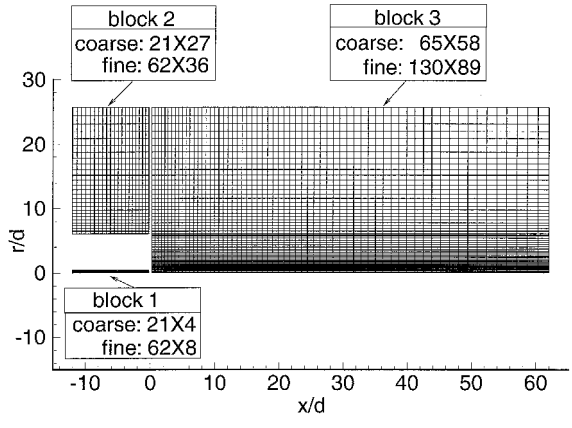

Fig. 2 Block decomposition of the solution domain (coarse mesh shown).

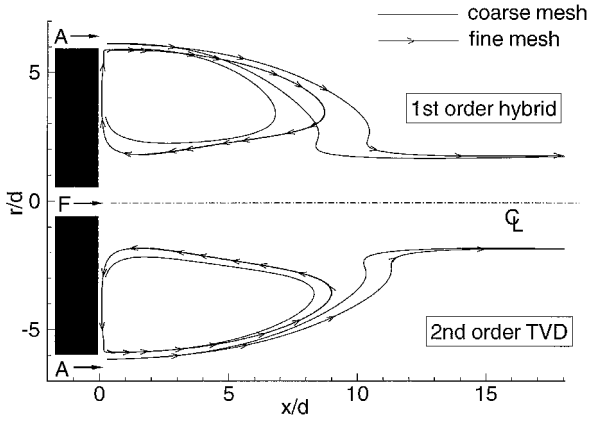

Fig. 3 Streamlines, comparison between the hybrid and the TVD schemes on two different meshes (flame A[4]).

Figure 4 shows the contour plot of the Favre mean mixture fraction obtained with the two-combustion model presented here. Figure 5 shows the Favre mean and rms/mean mixture fraction along the combustor axis, whereas Figs. 6 and 7 show their radial profiles at $x/d = 10$ and 20. Finally, Figs. 8 and 9 show the radial profiles of the Favre mean $\tilde{r}$ and the Favre cross-correlation $\widetilde{f''r''}$. The comparison with experiments, where available, is good.

From these figures it is possible to see that the presumed PDF and the PDF transport models give practically the same results, with the exception of $\widetilde{f''r''}$; this is not surprising, be-

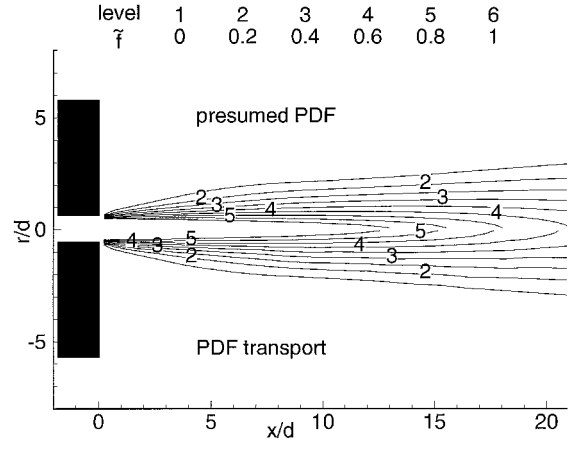

Fig. 4 Contour plot of $\tilde{f}$ obtained with the presumed PDF (upper half) and PDF transport methods (flame A[4]).

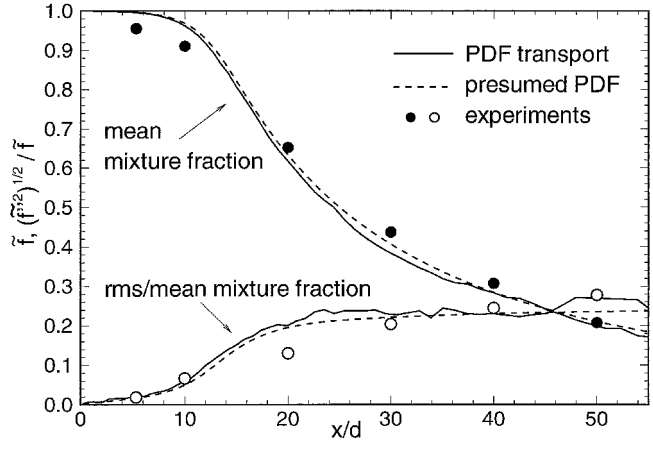

Fig. 5 Favre rms/mean mixture fraction along the combustor axis (flame A[4]).

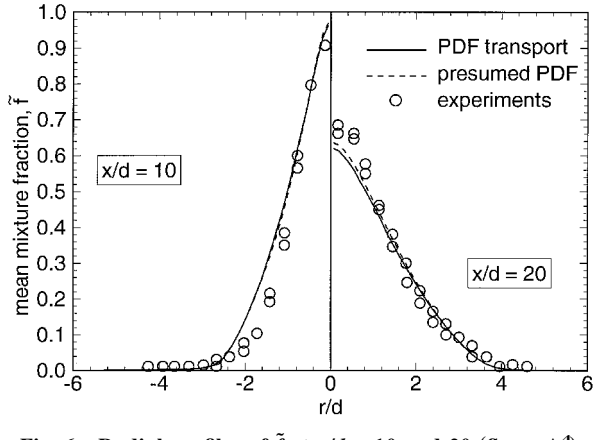

Fig. 6 Radial profiles of $\tilde{f}$ at $x/d = 10$ and 20 (flame A[4]).

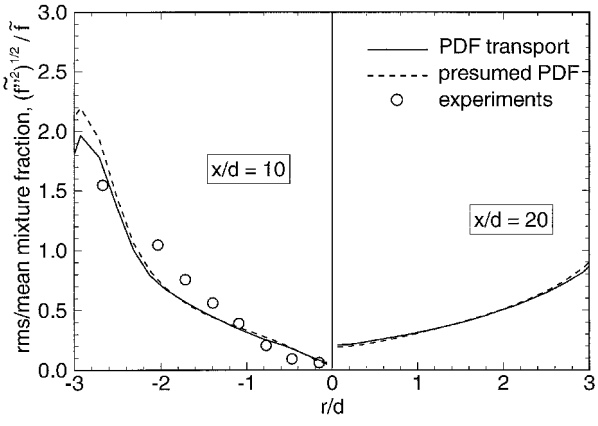

Fig. 7 Radial profiles of the Favre rms/mean mixture fraction at x/d = 10 and 20 (flame A[4]).

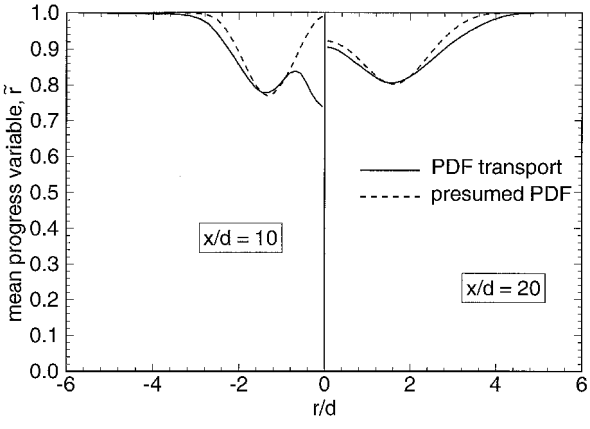

Fig. 8 Radial profiles of the Favre normalized progress variable at x/d = 10 and 20 (flame A[4]).

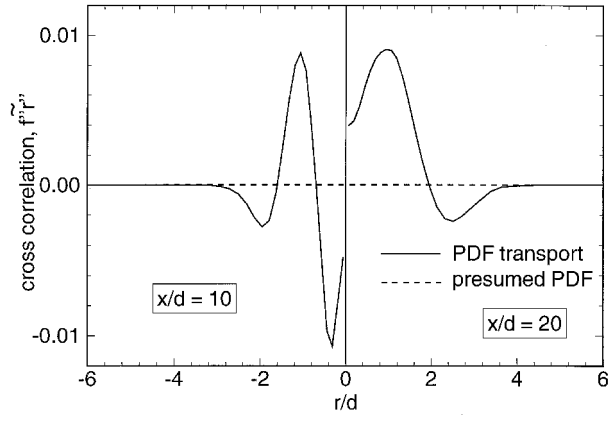

Fig. 9 Radial profiles of $\widetilde{f''r''}$ at x/d = 10 and 20 (flame A[4]).

cause PDF transport Eq. (21) has been modeled in such a way to give for $\tilde{f}$, $\widetilde{f''^2}$, $\tilde{r}$, $\widetilde{r''^2}$, when integrated, the same transport equations used in the presumed PDF method. This is not the case for the other statistical moments as Fig. 9 shows for $\widetilde{f''r''}$; in fact, $\widetilde{f''r''}$ is identically zero in the presumed PDF method because of the statistical independence hypothesis between f and r [see Eq. (13)]. The PDF transport method instead predicts a large correlation between f and r.

Figure 10 shows the Favre PDFs of the mixture fraction at three different points of the combustor. The two methods give comparable results, also for this quantity the irregular PDF obtained with the PDF transport method is because of the finite number of Monte Carlo particles.

The large difference in $\widetilde{f''r''}$ between the two methods doesn't seem to affect the mean thermochemical quantities, which are practically coincident. Figure 11 shows the conventional mean temperature radial profiles at x/d = 10 and 20. Also, in this case, the predictions obtained with the partial equilibrium model are in fair agreement with the experimental data, the maximum temperature being underpredicted of ≃200 K. The figure shows also the temperature profiles obtained under full thermochemical equilibrium conditions with 1) $\tilde{P}(f)$ assumed equal to the β function and 2) $\tilde{P}(f) = \delta(f - \tilde{f})$, i.e., without any turbulence–chemistry interaction model (quasilaminar approach). The difference in peak temperature between the two cases is about 300 K, showing that the effect of turbulent fluctuations on chemistry is not negligible; in case 1) the equilibrium temperature is higher than the partial equilibrium one because of the complete recombination of free radicals.

Figure 12 shows radial profiles of the CO mean mass fractions at x/d = 10 and 20. The agreement between the predictions and the experiments is good at x/d = 10 and only fair at x/d = 20, the centerline value at x/d = 20 being underpredicted; as already pointed out by Correa and Gulati,[4] this is because of the inadequacy of the partial equilibrium hypothesis for the two-body shuffle reactions in the rich part of the flame.

Finally, Fig. 13 shows radial profiles of the O mean mass fraction; the full equilibrium model gives a maximum value of the O mass fraction, which is nearly two orders of magnitude less than the one obtained accounting for the finite rate kinetics of radicals recombinations; therefore, considering that the thermal nitric oxide NO production rate depends linearly

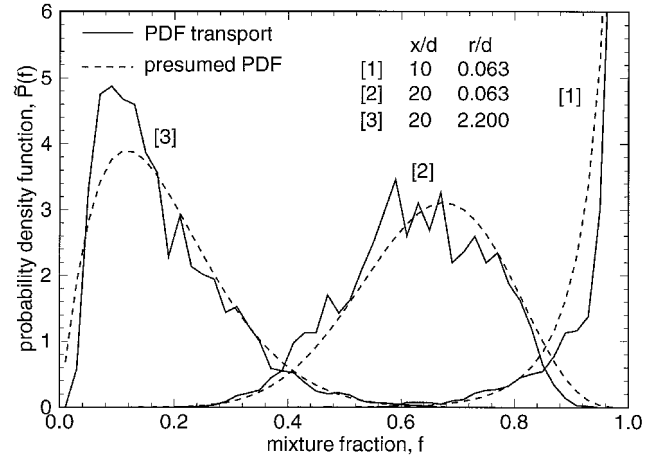

Fig. 10 PDFs at three different points of the combustor (flame A[4]).

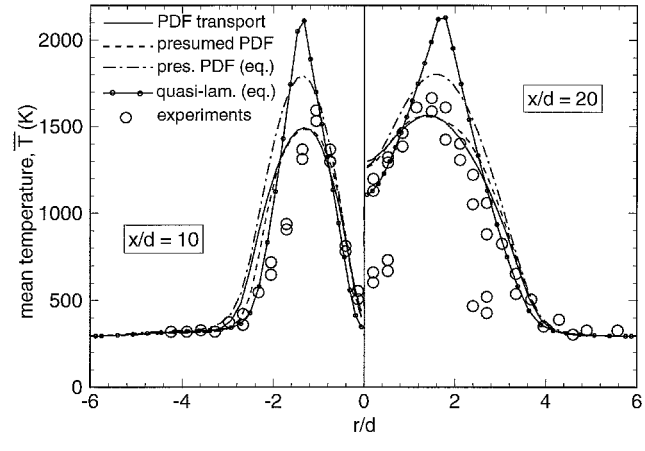

Fig. 11 Radial profiles of the mean temperature at x/d = 10 and 20 (flame A[4]).

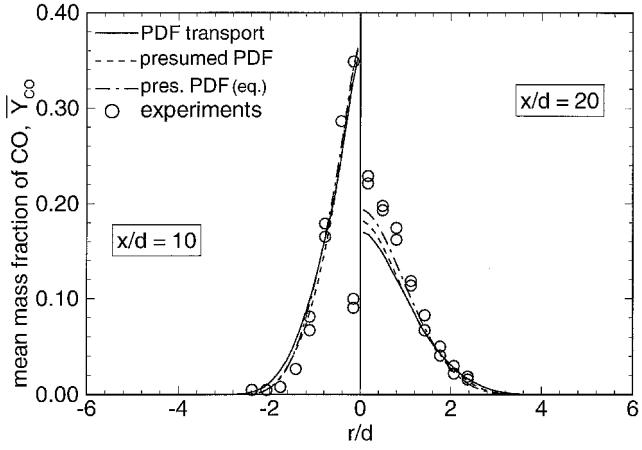

Fig. 12 Radial profiles of the CO mean mass fraction at *x/d* = 10 and 20 (flame A[4]).

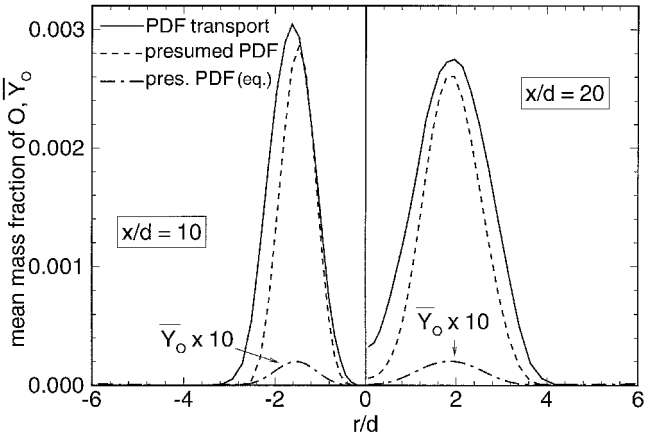

Fig. 13 Radial profiles of the O mean mass fraction at *x/d* = 10 and 20 (flame A[4]).

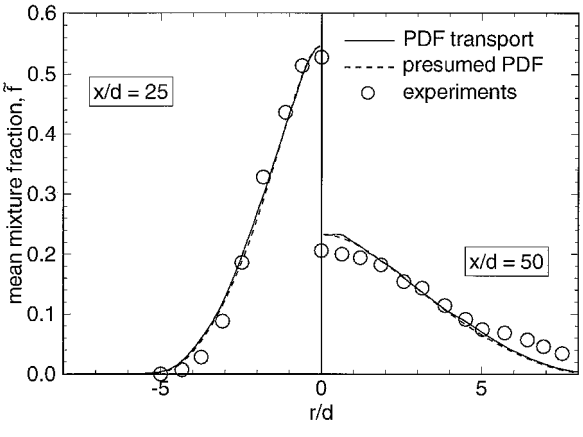

Fig. 14 Radial profiles of $\tilde{f}$ at *x/d* = 25 and 50 (flame B[5]).

on the oxygen concentration, it seems fair to conclude that it is important to account for superequilibrium concentrations of free radicals.

Flame B

Similar considerations hold for flame B. Figure 14 shows the radial profiles of the Favre mean mixture fraction at *x/d* = 25 and 50. The comparison with the experiments is good, the fuel–air mixing rate between the two sections being slightly underpredicted.

Figure 15 shows the radial profiles of mean temperature. The agreement of the results obtained with the partial equilibrium

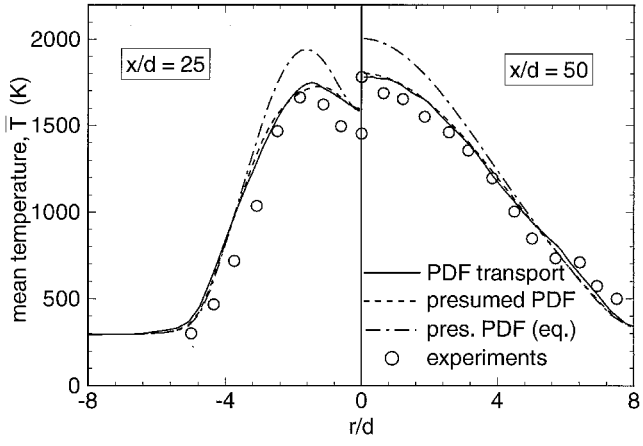

Fig. 15 Radial profiles of the mean temperature at *x/d* = 25 and 50 (flame B[5]).

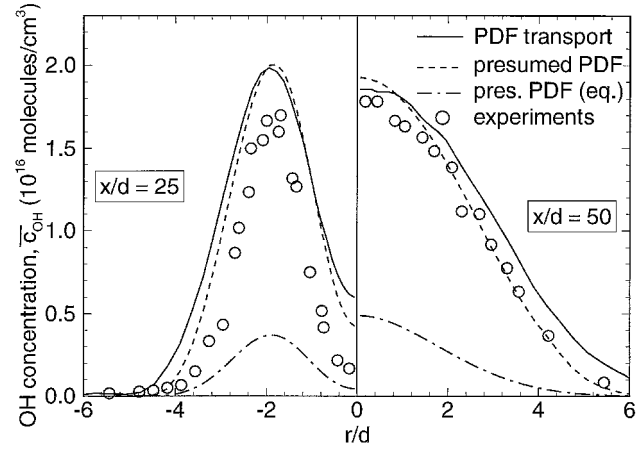

Fig. 16 Radial profiles of the OH mean concentration at *x/d* = 25 and 50.

model is good; note also that the use of the full equilibrium model gives a maximum temperature level that is ≃300 K larger than the experiments.

Finally, Fig. 16 shows the radial profiles of the OH concentration. The results obtained with the partial equilibrium model are in good agreement with the experiments, whereas the use of the full thermochemical equilibrium model gives a large error. Also, in this case, the importance of accounting for super equilibrium concentrations of free radicals is demonstrated.

Conclusions

The present work shows that the presumed PDF and the PDF transport methods with a thermochemical model based on a one-step reduced reaction mechanism where only finite rate kinetics of free radical recombinations is accounted for, give comparable results when used to simulate $H_2/CO/N_2$–air non-premixed turbulent flames; therefore, the application of presumed PDF methods for design applications is strongly recommended, their computational effort being nearly 20 times smaller than Monte Carlo PDF transport methods.

Note that PDF transport methods have a larger field of applicability than the one presented here. Including the velocity components among the PDF parameters, for example, results in an approach where turbulent transport is in closed form.[7] Furthermore, more than two independent thermochemical variables can be easily included to account for other important finite rate kinetics effects, e.g., ignition, that can be necessary for the simulation of more complex combustion problems (where the presumed PDF method may not be adequate), and

have been neglected here when assuming partial equilibrium for all two-body reactions.

In counterposition, the presumed PDF method is not as flexible as the PDF transport method, even if some interesting work has been recently published to extend the application of the β-PDF to any number of thermochemical variables.[19]

It has been shown that for flame A (characterized by a small recirculation zone downstream of a flameholder) that the second-order TVD scheme proposed by Jones[11] gives accurate results, even on coarse meshes, whereas the classical first-order hybrid scheme is negatively affected by numerical diffusion.

Finally, the importance of accounting for the superequilibrium concentrations of free radicals, that in the case of O have been found nearly two orders of magnitude larger than the equilibrium values, has been established.

Future work will address the application of the composition PDF transport method with more than one-step reduced reaction mechanisms to account for more finite rate kinetics effects. Parallelization of the Monte Carlo solver developed here will also be addressed.

Acknowledgment

This work was financially supported by the Sardinian Regional Government.

References

[1]Borghi, R., "Turbulent Combustion Modeling," *Progress in Energy and Combustion Science*, Vol. 14, 1988, pp. 245–292.

[2]Bilger, R. W., "Turbulent Flows with Nonpremixed Reactants," *Turbulent Reacting Flows I*, edited by P. A. Libby and F. A. Williams, Springer–Verlag, Heidelberg, 1980, pp. 65–112.

[3]Dopazo, C., "Recent Developments in PDF Methods," *Turbulent Reacting Flows II*, edited by P. A. Libby and F. A. Williams, Academic, London, 1992, pp. 375–474.

[4]Correa, S. M., and Gulati, A., "Measurements and Modeling of a Bluff Body Stabilized Flame," *Combustion and Flame*, Vol. 89, 1992, pp. 195–213.

[5]Drake, M. C., Pitz, R. W., Correa, S. M., and Lapp, M., "Nitric Oxide Formation from Thermal and Fuel-Bound Nitrogen Sources in a Turbulent Nonpremixed Syngas Flame," *Proceedings of the 20th Symposium (International) on Combustion* (Ann Arbor, MI), The Combustion Inst., Pittsburgh, PA, 1984, pp. 1983–1990.

[6]Janicka, J., and Kollmann, W., "A Two-Variables Formalism for the Treatment of Chemical Reactions in Turbulent H_2–Air Diffusion Flames," *Proceedings of the 17th Symposium (International) on Combustion*, The Combustion Inst., Pittsburgh, PA, 1979, pp. 421–430.

[7]Pope, S. B., "A Monte Carlo Method for the PDF Equations of Turbulent Reactive Flow," *Combustion Science and Technology*, Vol. 25, 1981, pp. 159–174.

[8]Biagioli, F., "Modeling Turbulent Combustion with PDF Methods," Ph.D. Dissertation, Dept. of Mechanics and Aeronautics, Univ. of Rome La Sapienza, Rome, Italy, Jan. 1995.

[9]Patankar, S. V., *Numerical Heat Transfer and Fluid Flow*, Hemisphere, New York, 1980.

[10]Rhie, C. M., and Chow, W. L., "Numerical Study of the Turbulent Flow past an Airfoil with Trailing Edge Separation," *AIAA Journal*, Vol. 11, 1983, pp. 1523–1532.

[11]Jones, W. P., "Turbulence Modelling and Numerical Solution Methods for Variable Density and Combusting Flows," *Turbulent Reacting Flows II*, edited by P. A. Libby and F. A. Williams, Academic, London, 1992, pp. 309–379.

[12]Tolpadi, A. K., and Correa, S. M., "A Monte Carlo PDF Method for the Calculation of Gas Turbine Combustor Flow Fields," AIAA Paper 95-2443, July 1995.

[13]Baurle, R. A., Hsu, A. T., and Hassan, H. A., "Assumed and Evolution Probability Density Functions in Supersonic Turbulent Combustion Calculations," *Journal of Propulsion and Power*, Vol. 11, 1995, pp. 1132–1153.

[14]Launder, B. E., and Spalding, D. B., "The Numerical Computation of Turbulent Flows," *Computational Methods in Applied and Mechanical Engineering*, Vol. 3, 1974, pp. 269–289.

[15]Warnatz, J., "Concentration-, Pressure- and Temperature-Dependence of the Flame Velocity in Hydrogen-Oxygen-Nitrogen Mixtures," *Combustion Science and Technology*, Vol. 26, 1981, pp. 203–213.

[16]Gordon, S., and McBride, B. J., "A Computer Program for Calculation of Complex Chemical Equilibrium Composition," NASA SP-273, Feb. 1971.

[17]Janicka, J., and Kollmann, W., "The Calculation of Mean Radical Concentrations in Turbulent Diffusion Flames," *Combustion and Flame*, Vol. 44, 1982, pp. 319–336.

[18]Dopazo, C., "PDF Approach for a Turbulent Axisymmetric Heated Jet: Centerline Evolution," *Physics of Fluids*, Vol. 18, 1975, pp. 397–404.

[19]Girimaji, S. S., "Assumed β-pdf Model for Turbulent Mixing: Validation and Extension to Multiple Scalar Mixing," *Combustion Science and Technology*, Vol. 78, 1991, pp. 177–196.